

## On the Relationship between Stratiform Low Cloud Cover and Lower-Tropospheric Stability

ROBERT WOOD AND CHRISTOPHER S. BRETHERTON

*University of Washington, Seattle, Washington*

(Manuscript received 25 January 2006, in final form 12 May 2006)

### ABSTRACT

Observations in subtropical regions show that stratiform low cloud cover is well correlated with the lower-troposphere stability (LTS), defined as the difference in potential temperature  $\theta$  between the 700-hPa level and the surface. The LTS can be regarded as a measure of the strength of the inversion that caps the planetary boundary layer (PBL). A stronger inversion is more effective at trapping moisture within the marine boundary layer (MBL), permitting greater cloud cover. This paper presents a new formulation, called the *estimated inversion strength* (EIS), to estimate the strength of the PBL inversion given the temperatures at 700 hPa and at the surface. The EIS accounts for the general observation that the free-tropospheric temperature profile is often close to a moist adiabat and its lapse rate is strongly temperature dependent. Therefore, for a given LTS, the EIS is greater at colder temperatures. It is demonstrated that while the seasonal cycles of LTS and low cloud cover fraction (CF) are strongly correlated in many regions, no single relationship between LTS and CF can be found that encompasses the wide range of temperatures occurring in the Tropics, subtropics, and midlatitudes. However, a single linear relationship between CF and EIS explains 83% of the regional/seasonal variance in stratus cloud amount, suggesting that EIS is a more regime-independent predictor of stratus cloud amount than is LTS under a wide range of climatological conditions.

The result has some potentially important implications for how low clouds might behave in a changed climate. In contrast to Miller's thermostat hypothesis that a reduction in the lapse rate (Clausius-Clapeyron) will lead to increased LTS and increased tropical low cloud cover in a warmer climate, the results here suggest that low clouds may be much less sensitive to changes in the temperature profile if the vertical profile of tropospheric warming follows a moist adiabat.

### 1. Introduction

Observations show that on daily to interannual time scales, stratiform low cloud fraction (CF) is strongly correlated with the lower-tropospheric stability (LTS), defined as the difference between the potential temperature  $\theta$  of the free troposphere (700 hPa) and the surface,  $LTS = \theta_{700} - \theta_0$  (Slingo 1987; Klein and Hartmann 1993; Klein 1997; Wood and Hartmann 2006).

Relationships between LTS and CF from observations in the Tropics (Slingo 1980) and subtropics (Klein and Hartmann 1993) have been used in the parameterization of low cloud cover in general circulation models (e.g., Slingo 1987; Rasch and Kristjansson 1998) used to

predict climate changes. They are also a key assumption in the thermostat hypothesis of Miller (1997) and in the climate sensitivity study of Larson et al. (1999). Both of these studies find a strong negative low cloud feedback on climate changes due to a marked increase in low cloud cover as the sea surface temperature (SST) increases. However, it has yet to be demonstrated whether the observationally derived LTS–CF relationships will hold in a changed climate.

Most cloud-topped boundary layers are convectively driven and have relatively weak internal stratification. In such situations, the LTS is mainly due to the potential temperature increase across the capping inversion and the accumulated static stability between this inversion and the 700-hPa reference level. High LTS is associated with strong, low-lying inversions for which both of these contributions are large. Physically, both factors promote a well-mixed, weakly entraining boundary layer in which there is efficient turbulent cou-

---

*Corresponding author address:* Dr. Robert Wood, Atmospheric Sciences, University of Washington, Box 351640, Seattle, WA 98195.

E-mail: robwood@atmos.washington.edu

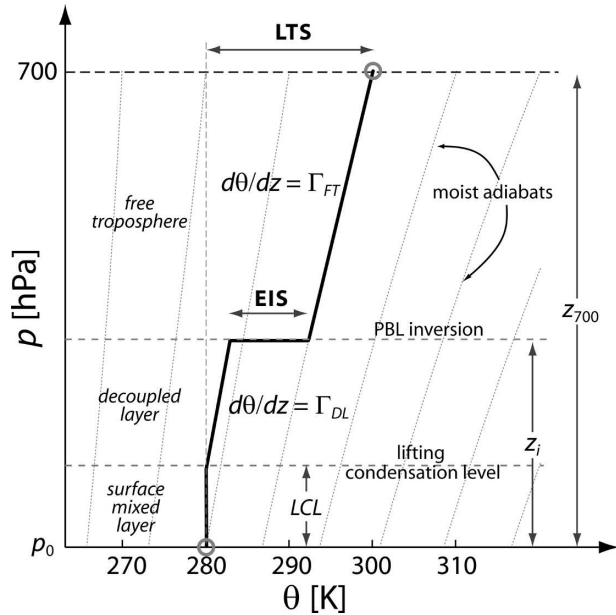


FIG. 1. Idealized profile (thick solid line) of lower-tropospheric structure during periods of undisturbed flow. Moist adiabats are shown as light dotted lines.

pling of a stratocumulus cloud layer with its surface moisture supply (Bretherton and Wyant 1997; Wyant et al. 1997).

The predictive success of LTS, which is a bulk measure of inversion strength, suggests that a more refined measure of inversion strength might be even more skillful. In this study we propose such a refinement of LTS, the estimated inversion strength (EIS), which we argue is an even better predictor of the planetary boundary layer (PBL) inversion strength and low cloud cover, especially under global climate changes. We test this refinement using rawinsonde profiles, reanalysis data, and surface observer cloud reports.

## 2. Relationship between lower-tropospheric stability and inversion strength

Figure 1 shows an idealized temperature profile for the lower troposphere ( $p > 700$  hPa) typical of periods of moderate tropospheric subsidence conducive to the formation of extensive low clouds. Turbulence primarily driven by strong PBL radiative cooling and cold advection results in a PBL that is capped by an inversion (often referred to as the trade inversion) at a height  $z_i$  with a strength  $\Delta\theta$  in the range of 1–10 K. Although the real structure in the PBL, inversion, and just above the inversion is more complex than shown in Fig. 1, this figure still provides a useful basis for relating LTS to inversion strength.

The PBL may be vertically well mixed (e.g., nocturnal coastal stratocumulus) or decoupled into multiple turbulent layers (e.g., trade cumulus). Two-layer bulk models have been proposed that can treat both PBL types reasonably accurately (e.g., Albrecht et al. 1979; Betts and Ridgway 1988; Park et al. 2004). These break the PBL into a surface mixed layer (SML), which is a well-mixed layer that extends from the surface to the surface-based lifting condensation level (LCL), and a decoupled layer (DL) that extends from the LCL to the PBL top in which the potential temperature increases approximately linearly with height at some rate  $\Gamma_{DL}$ . Above the PBL exists a free-tropospheric layer with a potential temperature that increases approximately linearly with height with a gradient  $\Gamma_{FT}$ . Using this simple structure, we can relate  $\Delta\theta$  to the potential temperature  $\theta_{700}$  at 700 hPa, the height of the  $p = 700$  hPa surface  $z_{700}$ , the potential temperature at the surface  $\theta_0$ , and the PBL depth  $z_i$  as follows:

$$\Delta\theta = (\theta_{700} - \theta_0) - \Gamma_{FT}(z_{700} - z_i) - \Gamma_{DL}(z_i - \text{LCL}). \quad (1)$$

The first term on the rhs in the parentheses is the LTS as defined above, and so Eq. (1) expresses mathematically the basis for LTS being a measure of the inversion strength. Indeed,  $\Delta\theta$  would be perfectly correlated with LTS provided that the other terms involving the free-tropospheric and decoupled layer  $\theta$  gradients remained constant. However, as we shall show, these terms actually vary quite systematically with  $\theta_0$ . This destroys the unique relationship between  $\Delta\theta$  and LTS. It also suggests our next task, which is to find simple estimates of the free-tropospheric and decoupled layer  $\theta$  gradients.

### a. Free-tropospheric lapse rate

First, we note that in the free troposphere, the observed temperature profile is typically close to a moist adiabat. The tropical atmosphere, with its weak Coriolis force, cannot support strong horizontal gradients in temperature (Sobel et al. 2001), so the free-tropospheric temperature profile in regions of subsidence in the Tropics is set by the regions of active deep convection, where the profile is close to being moist adiabatic (Stone and Carlson 1979). Even in the midlatitudes, the free-tropospheric thermal stratification remains quite close to a moist adiabat, although the reasons for this are somewhat more subtle and involve horizontal, as well as vertical, mixing (Schneider 2007).

Evidence that the free-tropospheric profiles are closely tied to the moist adiabat is presented in Fig. 2, which shows  $\Gamma_{FT} = d\theta/dz$  between 700 and 850 hPa as

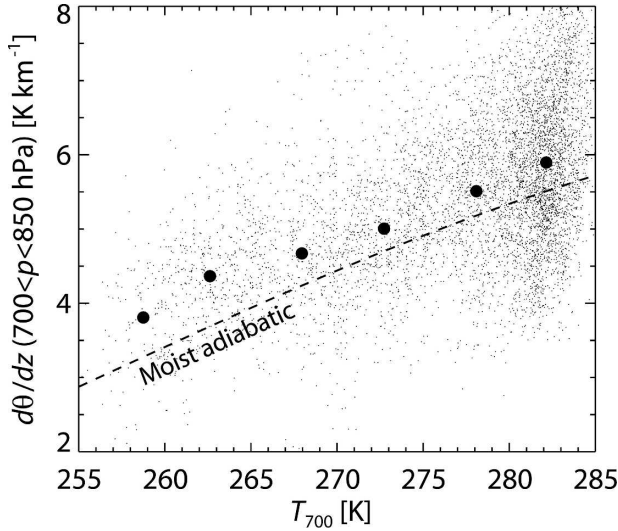


FIG. 2. Free-tropospheric lapse rate between 850 and 700 hPa estimated from  $2.5^\circ \times 2.5^\circ$  daily mean reanalysis data for 12 days (the first of each month) during 2003, plotted as a function of the temperature  $T_{700}$  at 700 hPa. Only data with daily mean 850-hPa subsidence rate in the range of  $0.2\text{--}0.8\text{ cm s}^{-1}$  are shown. The dots show the individual profiles and the solid circles are binned as a function of  $T_{700}$ . The dashed line shows the moist adiabatic lapse rate.

a function of the 700-hPa temperature. The data are taken from daily mean National Centers for Environmental Prediction–National Center for Atmospheric Research (NCEP–NCAR) reanalysis profiles (Kistler et al. 2001) with moderate subsidence (subsidence rate at 850 hPa in the range  $0.2\text{--}0.8\text{ cm s}^{-1}$ ) over the open oceans. Only profiles with surface temperatures  $270 < T_0 < 300\text{ K}$  and tropospheric relative humidity lower than 50% at 600–850 hPa are considered, so as to ensure an ice-free surface and a free troposphere without clouds. The results indicate that on average the free-tropospheric profiles tend to be close to, if slightly conditionally stable, with respect to the moist adiabat, a result that is in agreement with the zonal mean analysis of Schneider (2007).

Most important for the relationship between LTS and  $\Delta\theta$  is the systematic increase in  $\Gamma_{\text{FT}}$  with temperature that is a signature of the moist adiabat. Because  $\Gamma_{\text{FT}}$  is positively correlated with  $T_{700}$  (and hence  $\theta_{700}$ ), it is clear from Eq. (2) that LTS alone will not uniquely determine the inversion strength  $\Delta\theta$ .

### b. Decoupled layer $\theta$ gradient

The decoupled layer  $\theta$  gradient  $\Gamma_{\text{DL}}$  is dependent upon shallow convection and entrainment processes and depends in a nontrivial manner upon the moisture

structure in the lower troposphere. There is evidence that the vertical gradient of liquid potential temperature (conserved for moist processes) increases as the PBL depth increases, being close to zero for shallow, well-mixed (and stratocumulus capped) marine boundary layers (MBLs) to being close to a moist adiabat for deeper PBLs dominated by broken trade cumulus clouds (Albrecht et al. 1995; Park et al. 2004; Wood and Bretherton 2004).

When the PBL is shallow the value of  $\Gamma_{\text{DL}}$  is not particularly important in Eq. (1) because  $z_i - \text{LCL}$  is small. We therefore approximate  $\Gamma_{\text{DL}}$  by the moist adiabat passing through the LCL  $\Gamma_m(T_{\text{LCL}}, p_{\text{LCL}})$ . Here  $T_{\text{LCL}}$  and  $p_{\text{LCL}}$  are the temperature and pressure of the LCL, which are themselves only a function of the surface temperature, pressure, and relative humidity.

The decoupled layer  $\theta$  gradient  $\Gamma_{\text{DL}}$  has less leverage than  $\Gamma_{\text{FT}}$  on the relationship between LTS and  $\Delta\theta$  chiefly because the decoupled layer depth rarely exceeds 1 km, whereas  $z_{700} - z_i$  is rarely less than 1.5 km. This allows further simplification of Eq. (1) after it is rewritten in the form

$$\Delta\theta = (\theta_{700} - \theta_0) + z_i(\Gamma_{\text{FT}} - \Gamma_{\text{DL}}) - \Gamma_{\text{FT}}z_{700} + \Gamma_{\text{DL}}\text{LCL}. \quad (2)$$

We idealize  $\Gamma_{\text{FT}}$  as the slope of the moist adiabat through the 700-hPa temperature. The moist-adiabatic  $\theta$  gradients  $\Gamma_{\text{FT}}$  and  $\Gamma_{\text{DL}}$  do not differ by more than around  $0.8\text{ K km}^{-1}$ , which means that the term  $z_i(\Gamma_{\text{FT}} - \Gamma_{\text{DL}})$  in Eq. (2) will unlikely exceed  $1.6\text{ K}$  even for the deepest PBLs. Further, where observations suggest that  $z_i$  decreases with increased LTS (Wood and Bretherton 2004), values of  $\Gamma_{\text{FT}} - \Gamma_{\text{DL}}$  increase with LTS. Therefore, the contribution of this term to variability in the relationship between LTS and  $\Delta\theta$  is likely to be small, and will henceforth be neglected.

### c. A new measure of inversion strength

We are now in a position to define a new measure of inversion strength that incorporates an improved representation of the thermodynamic profile of the lower troposphere. In Eq. (2) we set  $z_i(\Gamma_{\text{FT}} - \Gamma_{\text{DL}}) = 0$ ,  $\Gamma_{\text{FT}} = \Gamma_m^{700} = \Gamma_m(T_{700}, 700\text{ hPa})$ , and  $\Gamma_{\text{DL}} = \Gamma_m^{\text{LCL}} = \Gamma_m(T_{\text{LCL}}, p_{\text{LCL}})$ . To determine the LCL we assume a constant surface relative humidity  $\text{RH}_0 = 0.8$  consistent with surface observations over subsiding regions of the oceans. We examine the sensitivity to this assumption below. We now define an estimated inversion strength EIS using Eq. (2), which is dependent only upon the temperatures at 700 hPa and at the surface, and (weakly) upon the surface pressure  $p_0$ :

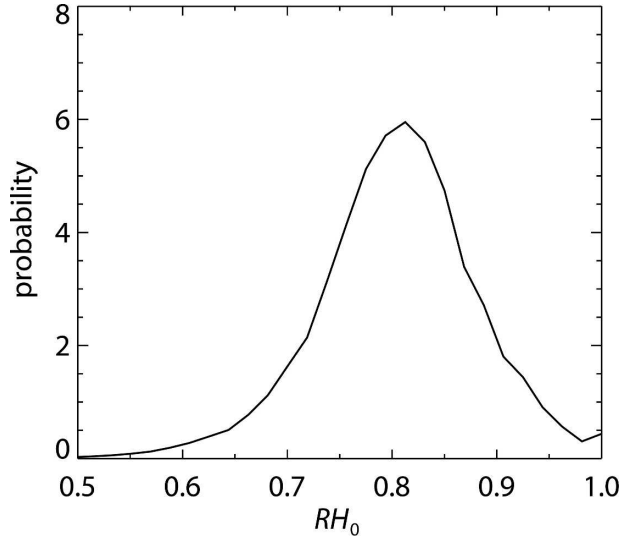


FIG. 3. Probability density function of surface relative humidity  $RH_0$  from COADS data over the global oceans, 60°S–60°N.

$$\text{EIS} = \text{LTS} - \Gamma_m^{700} z_{700} + \Gamma_m^{\text{LCL}} \text{LCL}. \quad (3)$$

We find that our results are insensitive to further simplification of EIS by replacing the two moist adiabats  $\Gamma_m^{700}$  and  $\Gamma_m^{\text{LCL}}$  with a single moist adiabat at 850 hPa calculated using the mean of the surface and 700-hPa temperatures  $\Gamma_m^{850} = \Gamma_m([T_0 + T_{700}]/2, 850 \text{ hPa})$ , such that

$$\text{EIS} = \text{LTS} - \Gamma_m^{850}(z_{700} - \text{LCL}). \quad (4)$$

The moist-adiabatic potential temperature gradient  $\Gamma_m$  can be calculated readily as

$$\Gamma_m(T, p) = \frac{g}{c_p} \left[ 1 - \frac{1 + L_v q_s(T, p)/R_a T}{1 + L_v^2 q_s(T, p)/c_p R_v T^2} \right], \quad (5)$$

where  $L_v$  is the latent heat of vaporization,  $q_s$  is the saturation mixing ratio,  $R_a$  and  $R_v$  are the gas constants for dry and water vapor, respectively,  $g$  is the gravitational acceleration, and  $c_p$  is the specific heat of air at constant pressure. Standard procedures exist to calculate the LCL from  $T_0$ ,  $p_0$ , and  $RH_0$ . The pdf of  $RH_0$  as deduced from all Comprehensive Ocean–Atmosphere Data Set (COADS) observations (Woodruff et al. 1998) over the global oceans 60°S–60°N is shown in Fig. 3, which shows a relatively narrow spread of  $RH_0$  with a mean of 0.8 and a standard deviation of 0.07. Little correlation is found between  $RH_0$  and  $T_0$  (not shown).

To calculate  $z_{700}$ , little error is introduced by assuming an exponential decrease in pressure with height with a single scale height:

$$z_{700} = (R_a T_0 / g) \ln(p_0 / 700 \text{ hPa}). \quad (6)$$

We should note that the regional and seasonal differences between LTS and EIS are primarily driven by the variability in  $\Gamma_m^{850}$  rather than variations in the LCL or  $z_{700}$  [see Eq. (4)]. A further assumption that these latter two variables are constant could be made at this point, which would simplify the definition of EIS somewhat, but in this study we include their variability for completeness.

The relationship between EIS, LTS, and the surface and 700-hPa air temperatures  $T_0$  and  $T_{700}$ , respectively, is shown in Fig. 4. Table 1 presents details of a number of specific regions that will be examined in this study [identical to those in Klein and Hartmann (1993)]. It is clear from the figure and Table 1 that a considerable range of EIS can be obtained for a given value of LTS by varying the temperature. Although the annual mean LTS in the North Atlantic region (50°–60°N, 35°–45°W) is similar to that in the Canarian region (15°–25°N, 25°–35°W), the EIS is considerably larger because the surface temperature is approximately 15 K colder. Similarly, although the LTS is much larger in the Peruvian region (10°–20°S, 80°–90°W) than in the North Atlantic, the annual mean EIS is quite similar because the Peruvian air is warmer. The key insight here is that although there is a good interseasonal correlation at any one location between LTS and EIS, there is no one unique relationship. As we shall see in the next section, this has important implications for the relationship between LTS and stratus cloud amount.

Figure 4 also shows that the sensitivity of EIS to changes in  $RH_0$  and  $p_0$  within the range of observed values is actually quite small. Given that seasonal mean values of  $RH_0$  for the different regions are all in the range of 0.75–0.85, this variability is unlikely to influence the EIS by more than 1 K or so. The effect upon EIS of reasonable pressure variations is even weaker.

So far, although we have presented theoretical arguments and some evidence that EIS should be an improved measure of the inversion strength  $\Delta\theta$  compared with LTS, we have not clearly demonstrated that EIS is truly a better measure of inversion strength. It is not possible to determine  $\Delta\theta$  directly from reanalysis data because of the poor vertical resolution, and so we turn to available observations that document the lower-tropospheric structure to give a range of surface temperature variability. Figure 5 shows that the EIS is indeed a better predictor of the inversion strength  $\Delta\theta$  over a wide range of temperatures. Taking the subtropical data alone, there is little advantage of EIS over LTS, but the addition of the tropical and wintertime midlatitude data demonstrate the greater utility of EIS at estimating the inversion strength during relatively undisturbed periods when low clouds dominate. The

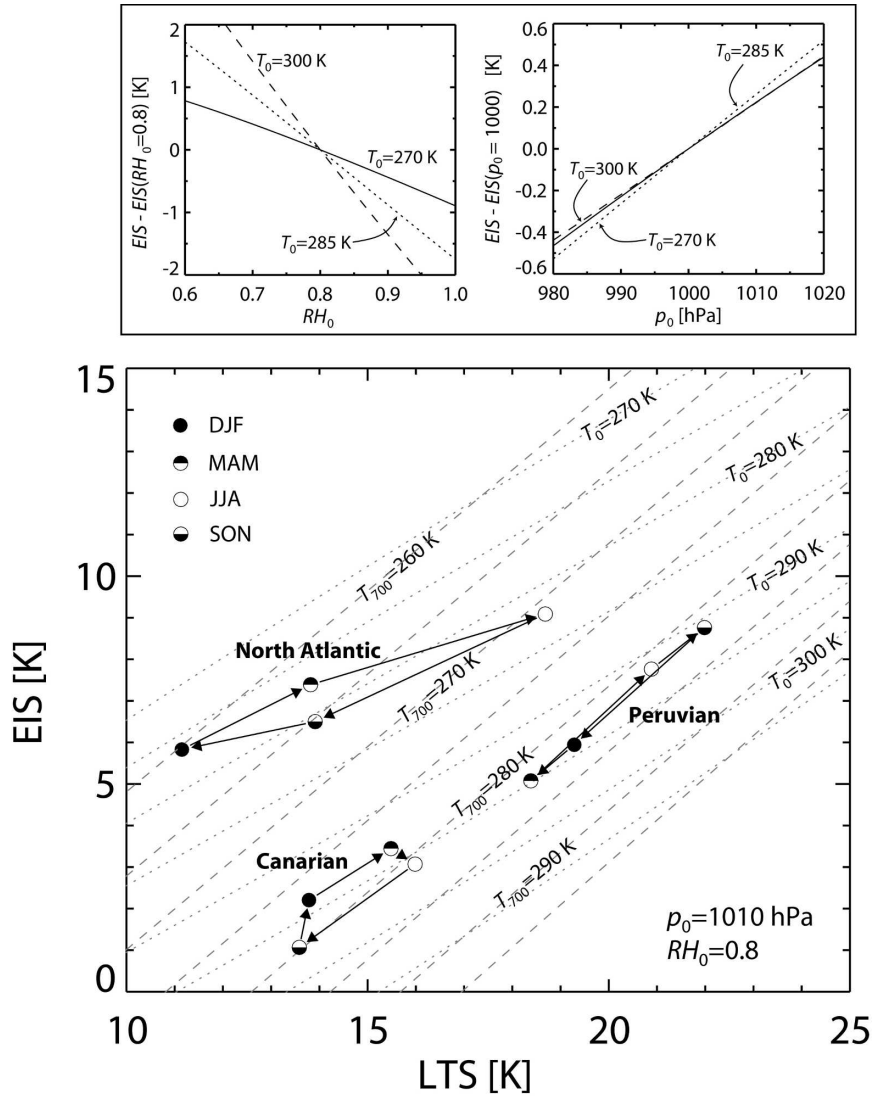


FIG. 4. Relationship between EIS and LTS for a range of surface air temperatures  $T_0$ . (bottom) Assumes  $p_0 = 1010$  hPa. (top) The sensitivity of EIS to changes in surface (left) relative humidity  $RH_0$  and (right) pressure  $p_0$ . Also shown are observationally derived values of EIS and LTS taken from NCEP reanalysis (again assuming  $RH_0 = 0.8$  and  $p_0 = 1010$  hPa) for seasons Dec–Feb (DJF), Mar–May (MAM), Jun–Aug (JJA), and Sep–Oct (SON), for three regions examined by Klein and Hartmann (1993; see Table 1 for locations).

TABLE 1. Details of the low cloud regions examined in this study. Note that these are identical to those used in Klein and Hartmann (1993).

Region	Symbol	Location	Type	Annual mean		
				LTS (K)	$T_0$ (K)	EIS (K)
Peruvian	P	10°–20°S, 80°–90°W	Tropical ocean	20.2	292.0	6.9
Namibian	N	10°–20°S, 0°–10°E	Tropical ocean	20.1	292.7	6.6
Californian	C	20°–30°N, 120°–130°W	Subtropical ocean	19.4	290.2	6.9
Australian	A	25°–35°S, 95°–105°E	Subtropical ocean	16.6	288.7	5.5
Canarian	Ca	15°–25°N, 25°–35°W	Subtropical ocean	14.7	294.3	2.5
North Pacific	Pa	40°–50°N, 170°E–180°	Midlatitude ocean	14.4	280.8	6.7
North Atlantic	At	50°–60°N, 35°–45°W	Midlatitude ocean	14.8	278.4	7.2
China	Ch	20°–30°N, 105°–120°E	Subtropical land	15.9	294.4	3.2

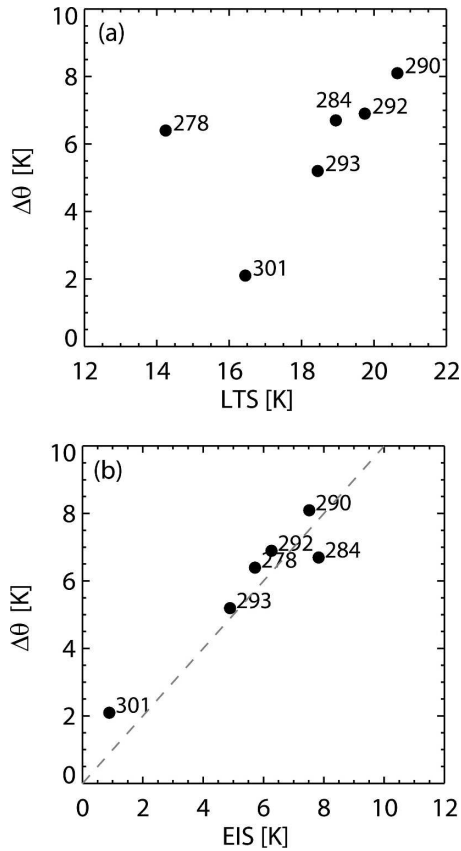


FIG. 5. Relationship between (a) mean LTS and mean inversion strength  $\Delta\theta$ ; and (b) mean EIS and mean  $\Delta\theta$ . Mean surface air temperatures ( $T_0$ , K) are shown next to the data points. Data are taken from times/regions dominated by low cloud conditions using composite inversion-normalized profiles obtained from the tropical east Pacific (Albrecht et al. 1995;  $T_0 = 301$  K), the southeast Pacific stratocumulus region at  $20^\circ\text{S}$ ,  $85^\circ\text{W}$  (Bretherton et al. 2004;  $T_0 = 290$  K), from ocean weather ship N in the subtropical northeast Pacific (Klein 1997;  $T_0 = 292$  K for large cloud amount composite and  $T_0 = 293$  K for small cloud amount composite), and from periods that stratocumulus clouds were prevalent at ocean weather ship C in the midlatitude North Atlantic (Norris 1998;  $T_0 = 284$  K for JJA and  $T_0 = 278$  K for DJF).

behavior of the LTS –  $\Delta\theta$  relationship is consistent with the greater values of  $\Gamma_{\text{FT}}$  in warmer conditions, that is, the trend toward weaker inversions for a given LTS, shown in Fig. 4.

### 3. Lower-tropospheric thermodynamics and low stratiform cloud amount

Klein and Hartmann (1993) found a linear relationship between seasonal mean LTS and low cloud amount for regions in the subtropics. Their data from regions other than the subtropics were not represented well by the linear relationship, as is shown in Fig. 6

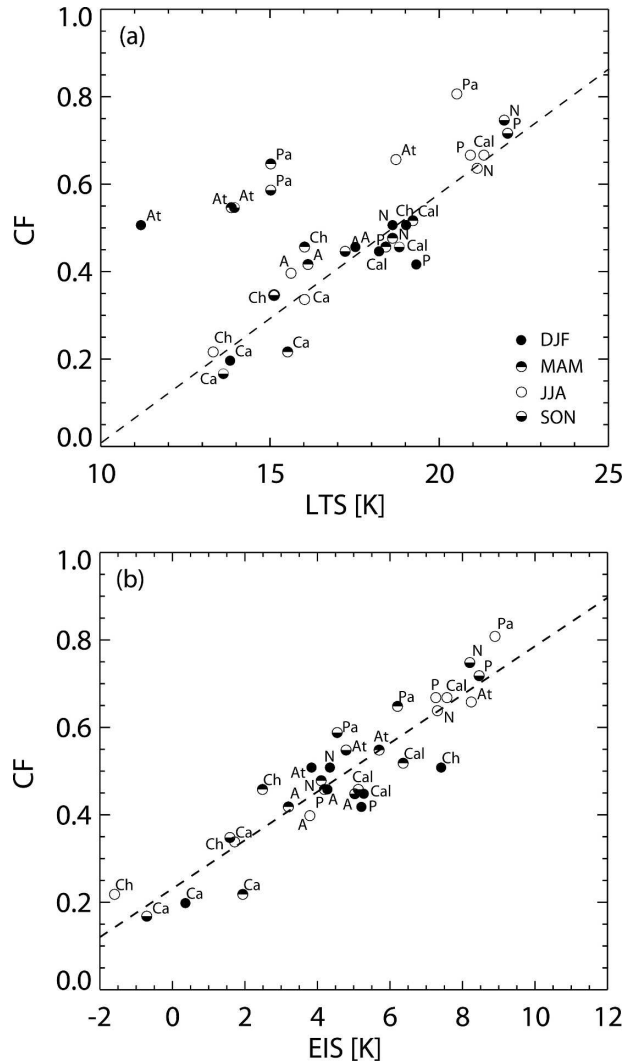


FIG. 6. Relationship between (a) LTS and low cloud amount, and (b) EIS and low cloud amount, for seasonal means at the locations described in Table 1. All seasons/regions where LTS > 10 K are plotted.

where we use NCEP reanalysis data for seasonal mean 700-hPa temperatures and other data where they were not provided in Klein and Hartmann (1993). Comparisons between the COADS–European Centre for Medium-Range Weather Forecasts (ECMWF) data used therein and the NCEP reanalysis data showed excellent agreement. Stratus cloud amount data are taken directly from Klein and Hartmann (1993), who used the cloud atlas data of Warren et al. (1986, 1988). Here, low stratiform cloud amount CF includes stratus, stratocumulus, fractocumulus, fractostratus, and sky-obscuring fog. Cumulus clouds are not included. See Klein and Hartmann (1993) for further details of the cloud data used. In Fig. 6a, we clearly see that although there is a

good relationship between LTS and CF for the subtropical regions, this clearly breaks down for the midlatitude regions in the North Atlantic and Pacific, which tend to exhibit higher CF for a given LTS than their subtropical counterparts. It is true, however, that there is a good interseasonal correlation between LTS and CF in the midlatitude regions. Figure 6a shows that the EIS represents a much better predictor of CF across all regions and seasons than does LTS. The correlation coefficient between EIS and CF is 0.92. It is remarkable that a single metric depending only upon the surface and 700-hPa air temperatures is able to explain over 80% of the variance in the regional and seasonal stratus cloud amount covering regions from the Tropics to the midlatitudes. The best-fit linear relationship is  $CF = a + b \times EIS$ , where  $a = 0.14 \pm 0.06$  and  $b = 0.060 \pm 0.010 \text{ K}^{-1}$ , with the errors quoted at the 95% level.

#### 4. Discussion and implications

Stratus cloud amount scales extremely well with the EIS. Furthermore, the inversion strength is not uniquely related to the LTS. For a given LTS, the vertical gradient of potential temperature corresponding to the moist adiabat increases with increasing temperature, so that a reduced fraction of the LTS between 700 hPa and the surface is attributable to the sharp PBL inversion at warmer temperatures. We should note here that this behavior is to a certain extent captured by the low cloud parameterization of Betts and Boers (1990), but additional information is required in this parameterization about the free-tropospheric humidity, making it less attractive as a simple scaling measure.

How low clouds respond to changes in regional and global climate constitutes a major uncertainty in predictions of climate sensitivity (Bony and Dufresne 2005). Two recent model studies (Miller 1997; Larson et al. 1999), both based upon the idea that low cloud cover in the Tropics increases with lower-tropospheric stability, suggest that low clouds will increase markedly under a warmed climate and hence will constitute a major negative feedback on the climate system due to the enhanced albedo. In both of these studies perturbations in low cloud CF' and LTS' were assumed to be linearly related in accordance with the observations of Klein and Hartmann (1993). Insofar as the results presented here are applicable to a future climate, they are suggestive of a much weaker response of low clouds in a warmed climate than in the two-box model studies (Miller 1997; Larson et al. 1999) that are based on the Klein–Hartmann LTS–CF regression. If the surface air temperatures warm more or less evenly in the tropical warm pool and the regions of low cloud surrounding

them, we would expect LTS to increase because of the behavior of the moist adiabat with increasing temperature. The enhanced cloud fraction predicted by the regression produces a marked negative feedback on climate changes in these models.

If the aforementioned models were to have used an EIS-based regression for cloud fraction of the form  $CF' \propto EIS'$ , they would have produced a much weaker low cloud feedback. A rough calculation for  $T_0 = 285 \text{ K}$ , gives  $EIS' \approx 0.75T'_{700} - T'_0$ . Assuming that future changes in the lower troposphere follow a moist adiabat would lead to  $T'_{700} \approx 1.3T'_0$  based upon a linearization around  $T_0 = 285 \text{ K}$ . It is hardly surprising, given the moist adiabat features in the definition of EIS, that the resulting change in EIS is therefore close to zero. It would be interesting to apply the  $CF' \propto EIS'$  approximation in an energy balance model of climate feedbacks, but this is beyond the scope of this study. It would also be interesting to examine the hypothesis that small, climatic perturbations in low cloud amount are indeed correlated with fluctuations in EIS using equilibrium simulations using a large eddy model.

#### 5. Conclusions

In this paper we have presented a new estimate of the PBL inversion strength (the sharp jump in potential temperature  $\Delta\theta$  that caps the PBL) that is dependent only upon the temperatures at 700 hPa and at the surface. We refer to the new measure as the *estimated inversion strength* (EIS). An inversion atop the PBL is almost always present in undisturbed conditions in the Tropics, subtropics, and midlatitudes. We demonstrate using observations that the EIS is a more appropriate measure of  $\Delta\theta$  across a wider temperature range of temperatures. Further, it is shown that the correlation between seasonal/regional mean low cloud amount CF and EIS is considerably higher than with lower-tropospheric stability (LTS), especially in the radiatively important midlatitude oceanic stratus regimes. This calls into question the applicability of relationships between LTS and CF for use in predicting how low cloud cover will respond in a warmed climate. We hypothesize that EIS will be a better predictor of the low cloud response and could be incorporated into parameterizations for simple energy balance models.

*Acknowledgments.* This work was supported by NASA EOS Grant NAGS5-10624 and NSF grant ATM-0336703. The authors also wish to thank Stephen Klein for helpful discussions. We are grateful to Alan Betts and an anonymous reviewer for insightful comments.

## REFERENCES

- Albrecht, B. A., A. K. Berts, W. H. Schubert, and S. K. Cox, 1979: A model of the thermodynamic structure of the trade-wind boundary layer: Part I. Theoretical formulation and sensitivity tests. *J. Atmos. Sci.*, **36**, 73–89.
- , M. P. Jensen, and W. J. Syrett, 1995: Marine boundary layer structure and fractional cloudiness. *J. Geophys. Res.*, **100**, 14 209–14 222.
- Betts, A. K., and W. Ridgway, 1988: Coupling of the radiative, convective, and surface fluxes over the equatorial Pacific. *J. Atmos. Sci.*, **45**, 522–536.
- , and R. Boers, 1990: A cloudiness transition in a marine boundary layer. *J. Atmos. Sci.*, **47**, 1480–1497.
- Bony, S., and J.-L. Dufresne, 2005: Marine boundary layer clouds at the heart of tropical cloud feedback uncertainties in climate models. *Geophys. Res. Lett.*, **32**, L20806, doi:10.1029/2005GL023851.
- Bretherton, C. S., and M. C. Wyant, 1997: Moisture transport, lower-tropospheric stability, and decoupling of cloud-topped boundary layers. *J. Atmos. Sci.*, **54**, 148–167.
- , T. Uttal, C. W. Fairall, S. E. Yuter, R. A. Weller, D. Baumgardner, K. Comstock, and R. Wood, 2004: The EPIC 2001 stratocumulus study. *Bull. Amer. Meteor. Soc.*, **85**, 967–977.
- Kistler, R., and Coauthors, 2001: The NCEP/NCAR 50-year reanalysis: Monthly means CD-ROM and documentation. *Bull. Amer. Meteor. Soc.*, **82**, 247–267.
- Klein, S. A., 1997: Synoptic variability of low-cloud properties and meteorological parameters in the subtropical trade wind boundary layer. *J. Climate*, **10**, 2018–2039.
- , and D. L. Hartmann, 1993: The seasonal cycle of low stratiform clouds. *J. Climate*, **6**, 1588–1606.
- Larson, K., D. L. Hartmann, and S. A. Klein, 1999: The role of clouds, water vapor, circulation, and boundary layer structure in the sensitivity of the tropical climate. *J. Climate*, **12**, 2359–2374.
- Miller, R. L., 1997: Tropical thermostats and low cloud cover. *J. Climate*, **10**, 409–440.
- Norris, J. R., 1998: Low cloud type over the ocean from surface observations. Part I: Relationship to surface meteorology and the vertical distribution of temperature and moisture. *J. Climate*, **11**, 369–382.
- Park, S., C. B. Leovy, and M. A. Rozendaal, 2004: A new heuristic Lagrangian marine boundary layer cloud model. *J. Atmos. Sci.*, **61**, 3002–3024.
- Rasch, P. J., and J. E. Kristjansson, 1998: A comparison of the CCM3 model climate using diagnosed and predicted condensate parameterizations. *J. Climate*, **11**, 1587–1614.
- Schneider, T., 2007: The thermal stratification of the extratropical troposphere. *The Global Circulation of the Atmosphere*, T. Schneider and A. H. Sobel, Eds., Princeton University Press, in press.
- Slingo, J. M., 1980: A cloud parameterization scheme derived from GATE data for use with a numerical model. *Quart. J. Roy. Meteor. Soc.*, **106**, 747–770.
- , 1987: The development and verification of a cloud prediction scheme for the ECMWF model. *Quart. J. Roy. Meteor. Soc.*, **113**, 899–927.
- Sobel, A. H., J. Nilsson, and L. M. Pövlani, 2001: The weak temperature gradient approximation and balanced tropical moisture waves. *J. Atmos. Sci.*, **58**, 3650–3665.
- Stone, P. H., and J. H. Carlson, 1979: Atmospheric lapse rate regimes and their parameterization. *J. Atmos. Sci.*, **36**, 415–423.
- Warren, S. G., 1988: Global distribution of total cloud cover and cloud types over ocean. NCAR Tech. Note NCAR/TN-317 + STR, National Center for Atmospheric Research, Boulder, CO, 42 pp. + 170 maps.
- , C. J. Hahn, J. London, R. M. Chervin, and R. L. Jenne, 1986: Global distribution of total cloud cover and cloud types over land. NCAR Tech. Note NCAR/TN-273 + STR, National Center for Atmospheric Research, Boulder, CO, 29 pp. + 200 maps.
- Wood, R., and C. S. Bretherton, 2004: Boundary layer depth, entrainment, and decoupling in the cloud-capped subtropical and tropical marine boundary layer. *J. Climate*, **17**, 3576–3588.
- , and D. L. Hartmann, 2006: Spatial variability of liquid water path in marine boundary layer clouds: The importance of mesoscale cellular convection. *J. Climate*, **19**, 1748–1764.
- Woodruff, S. D., H. F. Diaz, J. D. Elms, and S. J. Worley, 1998: COADS Release 2 data and metadata enhancements for improvements of marine surface flux fields. *Phys. Chem. Earth*, **23**, 517–527.
- Wyant, M. C., C. S. Bretherton, H. A. Rand, and D. E. Stevens, 1997: Numerical simulations and a conceptual model of the stratocumulus to trade cumulus transition. *J. Atmos. Sci.*, **54**, 168–192.